HYDRODYNAMICS AND MORPHODYNAMICS IN THE SURF ZONE OF A DISSIPATIVE BEACH

Leo C. van Rijn[1], Dirk-Jan R. Walstra[2], Bart T. Grasmeijer[3] and Kees Kleinhout[4]

Abstract: Two profile models have been compared with field data measured at the Egmond sandy beach site (The Netherlands) within the framework of the European COAST3D project. Three hydrodynamic storm events and two morphodynamic events (storm and post-storm periods) have been selected for model comparison. The two profile models UNIBEST-TC and CROSMOR are process-based models; the UNIBEST-TC model is a deterministic model, whereas the CROSMOR model is probabilistic model based on a 'wave by wave' approach. The models show reasonable results for wave height, longshore current and offshore bar migration.

INTRODUCTION

Within the framework of the European COAST3D project field measurements of hydrodynamic parameters and detailed bathymetric surveys have been carried out in the tidal surf zone of Egmond beach (The Netherlands). The objectives of the COAST3D experiment are to collect field data for better understanding of the hydrodynamics of the surf zone and for evaluation of hydrodynamic and morphodynamic models. The data of the main campaign is used to evaluate two profile models. Model performance is evaluated both for hydrodynamic parameters and for morphological development.

COAST3D FIELD CAMPAIGN AT EGMOND (NL)

The Egmond site is located in the central part of the Dutch North Sea coast and consists of a sandy beach (about 0.3 mm sand) and two breaker bars. The beach width is about 125 m with a slope of about 1 to 40. The tidal range varies between 1.4 m

---

1) Professor, University of Utrecht, P.O. Box 80115, 3508 TC Utrecht, The Netherlands
2) Researcher, WL | Delft Hydraulics, P.O. Box 177, 2600 MH Delft, The Netherlands
3) Phd-student, University of Utrecht, P.O. Box 80115, 3508 TC Utrecht, The Netherlands
4) Msc-student, Delft University of Technology, P.O. Box 5048, 2600 GA Delft, The Netherlands.

and 2 m. The tidal peak currents in the offshore zone are about 0.5 m/s; the flood current to the north is slightly larger than the ebb current to the south.

Hydrodynamic process measurements have been carried out in an area of about 500x500 m^2 near the beach by use of instrumented tripods and poles. The objective was to determine the hydro-, sediment- and morphodynamic parameters on the time scale of a storm month focussing on the cross-shore gradients in the highly dynamic zone around the crest of the inner bar and to a lesser extent near the crest of the outer bar. Additional measurement stations were operated at or close to the boundaries (seaward, northern and southern) of the survey area to supply the boundary data of the wave and current fields.

Here the main transect is considered which is located at the tripod stations 1A to 1D. The field data measured in Stations 18A, 7A, and 2 are also used. These stations are supposed to be representative for the processes in the main transect, although not all stations (18A, 7A, 2) are located in the main transect. The location of the stations (in cross-shore direction) is shown in Figure 1.

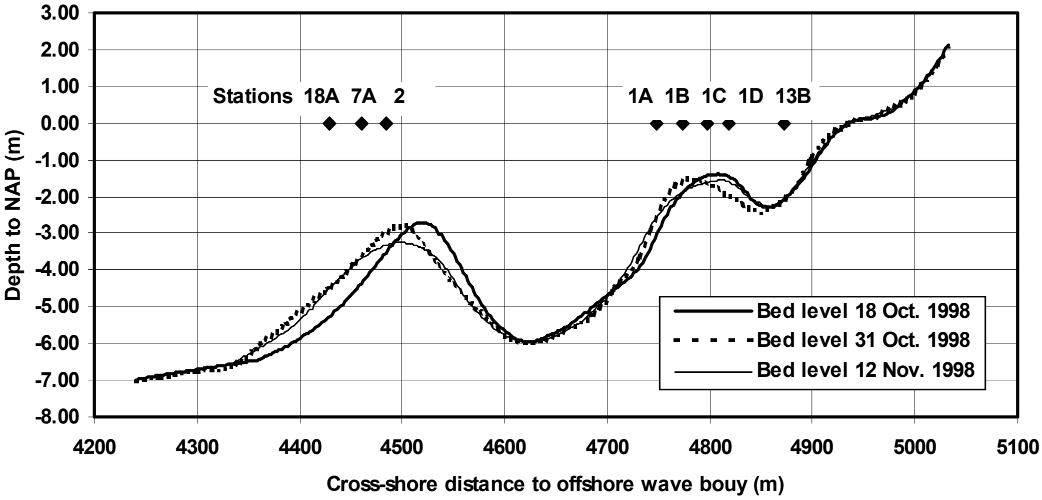

Figure 1 *Location of measurement stations during Main experiment October-November 1998: stations 1A, 1B, 1C, 1D and 13B are in main transect; stations 18A, 7A and 2 are about 300 m north of main transect.*

Station 7A is a fixed pole for wave height and water level measurements. Stations 18A and 13B are small frames for current velocity measurements (S4 instrument). Stations 2, 1A to 1D are tripods for wave height and velocity measurements. Background parameters of interest are the water temperature, which varied between 9 and 12 °C and the salinity, which varied between 20 and 25 promille. The maximum wind speed was about 20 m/s (Beaufort 8) from western directions (normal to shore) on 29 October. The wind and waves generally were in the same directions.

DESCRIPTION OF PROFILE MODELS

Two types of profile models (UNIBEST-TC and CROSMOR) both are designed to compute cross-shore sediment transport and the resulting profile changes under the combined action of waves, longshore tidal currents and wind. Both models consist of sub-modules in which the cross-shore distribution of waves, current velocities, sediment transport and the resulting profile changes are computed. Here, only the main differences between the models are discussed, a complete description of UNIBEST-TC and CROSMOR can be found in Bosboom et al. (1997) and van Rijn (2000) respectively.

The wave model in UNIBEST-TC is the well known Battjes and Janssen (1978) model, extended with a roller model (Nairn et al., 1990). The CROSMOR model is a probabilistic model based on the propagation and transformation of individual waves (wave by wave approach). Both transport modules are based on TRANSPOR (van Rijn, 1993). However, CROSMOR has the latest improvements of the transport formulations included (van Rijn, 2000).

Set-Up of Models

The models use the measured bottom profile of 26 October as the initial profile for the hydrodynamic runs. The various physical and model parameters were set at their default values. To account for inevitable measurement errors and variations, it was decided to perform a large number of hydrodynamic simulations in which the physical parameters were varied according to the (estimated) range of the measurement variations (in boundary conditions). Also, the model parameters such as the roughness height and wave breaker parameter γ were varied within site-specific valid ranges to obtain a range of model predictions. In the figures below an envelope of model results is shown for the hydrodynamic runs. If this range of model predictions falls within the error bands of the measurements this is considered as good agreement.

COMPARISON WITH MEASUREMENTS

Hydrodynamic Simulations

Three events have been selected for comparison of model results (
Table **1**).

Table 1 *Offshore boundary conditions.*

Event	*Wave height H_s (m)*	*Wave period T_p (s)*	*Wave angle (deg.) rel. to coast normal*	*Water level (m) to NAP*
28-10-1998 08:00	3.16	8.3	24	1.41
28-10-1998 16:00	3.91	8.3	-6	0.55
28-10-1998 23:00	4.55	10	3	1.59

In Figure 2 (top graph) the cross-shore distribution of the wave height is compared. Overall agreement for both models is acceptable, at the offshore bar agreement is good (x=4500m). However, at the inner breaker bar (x=4800m) both models are unable to predict the observed reduction in wave height. The CROSMOR model seems to perform somewhat better in this region, which is probably due to the application of the ‘wave by wave’ approach in combination with a cross-shore varying breaker function (γ), whereas UNIBEST-TC only represents the H_{rms} and a constant γ-value derived from the offshore wave conditions.

In the second graph of Figure 2 the (depth-averaged) longshore velocities are compared. The CROSMOR model over-estimates the longshore velocities on top of the two bars, whereas UNIBEST-TC under-estimates the longshore velocities across the complete profile. The higher longshore velocity values of CROSMOR on top of the bar are caused by the increased wave reduction at the two bars compared to UNIBEST-TC. The deviation in deeper water between the models is caused by the fact that CROSMOR uses the measured longshore velocities at Station 18A to derive the longshore pressure gradient, whereas UNIBEST-TC has the tide effect included by prescribing the longshore water surface gradient based on measured water levels in two stations alongshore (spacing of 30 km). Principally, this latter method is better, but it does not lead to better results, probably because inertia effects are not taken into account. The cross-shore currents are shown in the third graph of Figure 2. The performance of both models is poor. Neither is able to predict the large offshore-directed return flow both at the outer bar and inner bar. Deviations are most likely caused by the presence of a rip current at the main transect which results in increased offshore velocities which the profile models can not account for. The bottom graph of Figure 2 compares the peak orbital velocities (CROSMOR only) which are used to determine the cross-shore sediment transport due to wave asymmetry. Both the onshore and offshore-directed orbital velocities (based on the modified Isobe-Horikawa method, 1982) are reasonably predicted. At the two most landward stations on the inner bar the onshore-directed orbital velocities are significantly over-estimated. This again can be attributed to the model's inability to predict the rapid reduction in wave height in this region.

In Figure 3 (identical layout as Figure 2) the model results are compared for Event 2. Similar conclusions can be drawn as for Event 1. Again, both models are unable to predict the rapid decrease in wave height at the inner bar. The agreement of the longshore currents predicted by CROSMOR is significantly better compared to UNIBEST-TC. The cross-shore current at the inner bar is reasonably well simulated by the CROSMOR model; both models fail to simulate the rather large cross-shore current correctly at the outer bar.

Event 3 (Figure 4) has the highest wave height with an approximate coast normal incident wave angle. The longshore currents due tide, wind and wave effects are quite variable with northward-directed currents (wind and tide) at the outer bar and relatively small (0.1 to 0.2 m/s) southward-directed currents at the inner bar. The model results are rather sensitive to the wind and wave directions at small incident angles as can be seen from the relatively wide variation bands. It can be concluded that the models have not much predicting capabilities at small incident angles (<5 degrees). The maximum cross-shore currents are measured at the shoreward slope of the inner bar. Both models predict the maximum return flow on top or on the seaward slope of the inner bar. This is a typical result, which is often found in comparisons with laboratory experiments as well. The model results are at best reasonable at the inner bar.

Morphodynamic Simulations

The morphodynamic simulations are selected on the basis of the wave conditions between 18 October and 23 November 1998 of the main experiment, which can be roughly divided in: a) pre-storm period between 18-24 October: 3 minor storm events with $H_{s,o}$ up to 3 m; b) major storm period between 24 and 31 October: rapid succession of 4 major storm events with $H_{s,o}$ up to 5 m and c) post-storm period between 31 October-23 November: 1 major storm event with $H_{s,o}$ up to 4 m and 2 minor storm events with $H_{s,o}$ up to 2 m.

The storm period of 24-31 Oct. and the post-storm of 31 Oct.-12 Nov. have been selected for morphodynamic simulations.

The cross-shore profiles at Egmond are characterised by two bars: an outer breaker bar (at -2.5 m NAP) and an inner breaker bar (at -1 m NAP) with a cross-shore spacing of about 250 m. On large alongshore scale (10 km) and on long term (years), the behaviour of the outer and inner bars is 2-dimensional in the sense that the bars are continuous and of the same form in alongshore direction and show the same overall migrational pattern (onshore and offshore migration). On small scale (1 km) and on the short time scale of a storm month, alongshore non-uniformities may develop as local disturbances (rip channels, crescentic and meander patterns) which are superimposed on the overall straight base pattern yielding a 3-dimensional morphological system. The inherent spatial variability in longshore direction has been reduced by longshore-averaging of the available cross-shore profiles to obtain a longshore-averaged cross-shore profile for each date. These latter profiles have been used for model simulations. The basic overall features of the bars at the Egmond site are (see Figures 5 and 6):

- 24-31 Oct. (major storm period): significant offshore migration of outer bar and inner bar;
- 31 Oct.-12 Nov. (minor storm period): slight onshore migration of inner bar mainly due to bores produced after wave breaking at low tide conditions with water depths of about 1 m; no movement of outer bar.

The model results based on default values are shown in Figures 5 and 6. The current-related bed roughness is assumed to be $k_{s,c}$=0.03 m and the wave-related bed roughness is $k_{s,w}$=0.01 m. The bed material size is: d_{50}=0.00024 m and d_{90}=0.00048 m. Both models yield offshore migration of the outer and inner bars for the storm period of 24-31 Oct. The UNIBEST-TC model shows better agreement at the outer bar zone, whereas the CROSMOR model yields better results at the inner bar zone and the beach (Figure 5).

The model results for the post-storm period of 31 Oct.-12 Nov. are shown in Figure 6. As can be observed, the CROSMOR model yields slight onshore migration of the inner bar (erosion at seaward flank and deposition at landward flank), although the bar is also flattened. The UNIBEST-TC model yields offshore migration of the inner bar, which is most probably caused by the dominating effect of the undertow causing offshore transport, whereas the onshore-directed suspended transport is not taking into account. This latter wave-related suspended transport component is taken into account by the CROSMOR-model. This model also yields offshore migration of the inner bar, if the wave-related suspended transport is set to zero.

CONCLUSIONS

The main conclusions of the present study are:

- profile models can reasonably well predict the cross-shore wave height distribution; provided that the γ-breaker function is related to local parameters; the ‘wave by wave’ approach may better represent the wave height gradients over the inner bar crest;
- profile models can reasonably well predict the cross-shore distribution of the longshore current, provided that the wave incidence angle is relatively large (>5 degrees) and that the current velocity at the edge of the surf zone is known for calibration;
- profile models can not predict the cross-shore distribution of the undertow with sufficient accuracy; the field data are strongly affected by local circulation effects (rip currents);
- profile models can predict the offshore bar migration during major storm events;
- profile models can predict the onshore bar migration during post-storm events, provided that the onshore-directed wave-related suspended transport is modelled.

ACKNOWLEDGEMENTS

This work has been jointly funded by: a) National Institute for Coastal Zone Marine Management (RIKZ) of Rijkswaterstaat within the Generic Coastal Research Programme VOP 2000-2004, b) EU-sponsored MAST-3 COAST3D project under contract MAS3-CT97-0086 and, c) Delft Cluster Project Coasts contract 03.01.03.

REFERENCES

Battjes, J.A. and Janssen, J.P.F.M. 1978. Energy loss and set-up due to breaking waves in random waves. *16th Int. Conf. On Coastal Eng., ASCE, pp. 569-587.*

Bosboom, J., Aarninkhof, S.G.J., Reniers, AJ.H.M., Roelvink, J.A. and Walstra, D.J.R. 1997. Unibest-TC 2.0; Overview of model formulations. *WL|Delft Hydraulics report H2305.42, Delft, The Netherlands.*

Isobe, M and Horikawa, K. 1982. Study on water particle velocities of shoaling and breaking waves. *Coastal Engineering in Japan. Vol. 25.*

Nairn, R.B., Roelvink, J.A. and Southgate, H.N. 1990. Transition zone width and implications for modelling surfzone hydrodynamics. *Proceedings of the Int. Conf. Coastal Engineering Conference, Delft, The Netherlands, pp. 68-82.*

Van Rijn, L.C. 1993. Principles of sediment transport in rivers, estuaries and coastal seas. *Aqua Publications, Amsterdam, The Netherlands.*

Van Rijn, L.C., 2000. General view on sand transport by currents and waves. *WL|Delft Hydraulics Report Z2899.20/Z2099.30/Z2824.30, Delft.*

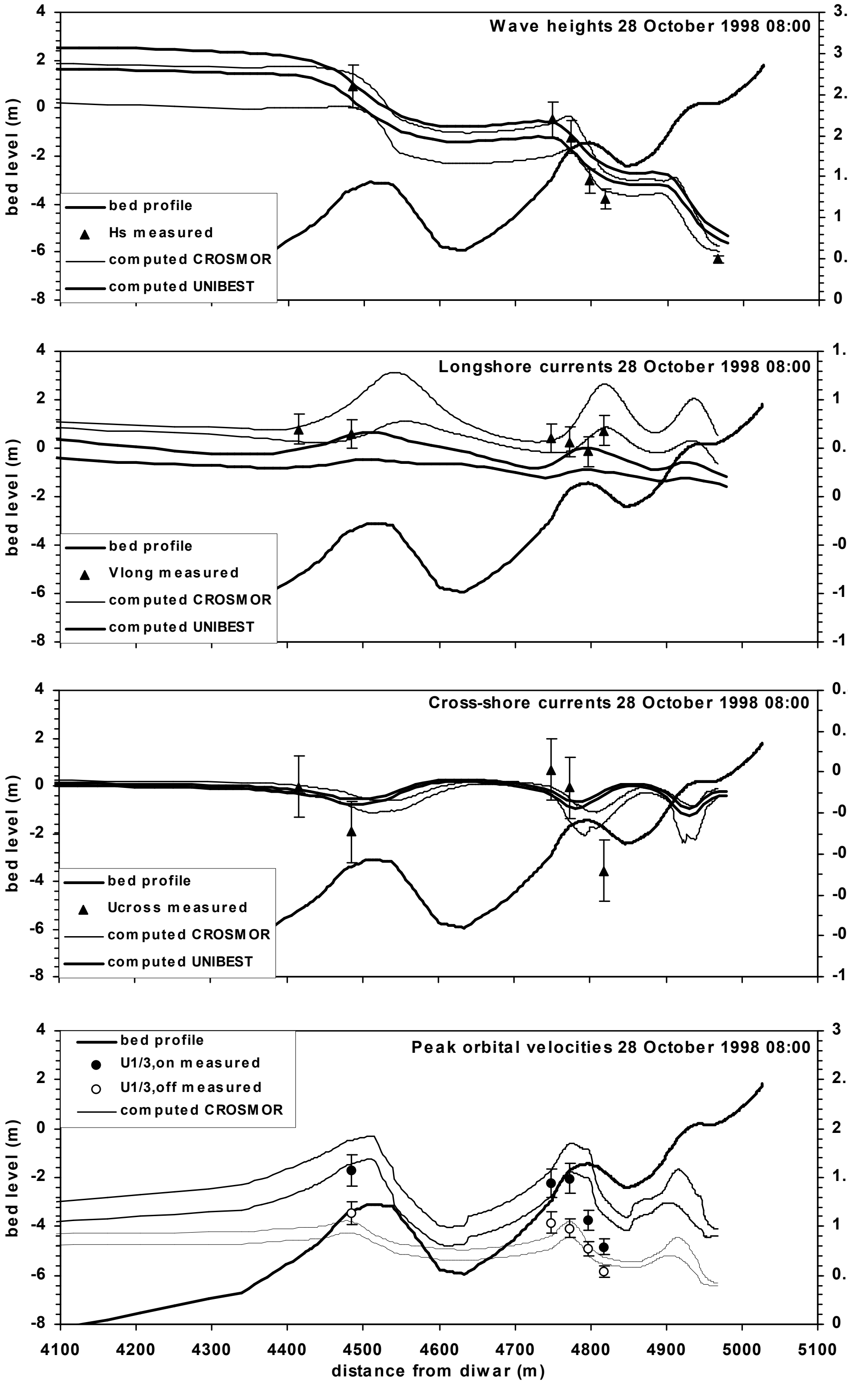

Figure 2 *Comparison of cross-shore distributions of wave height, longshore velocity and cross-shore velocity for Event 1 (28-10-1998 9:00).*

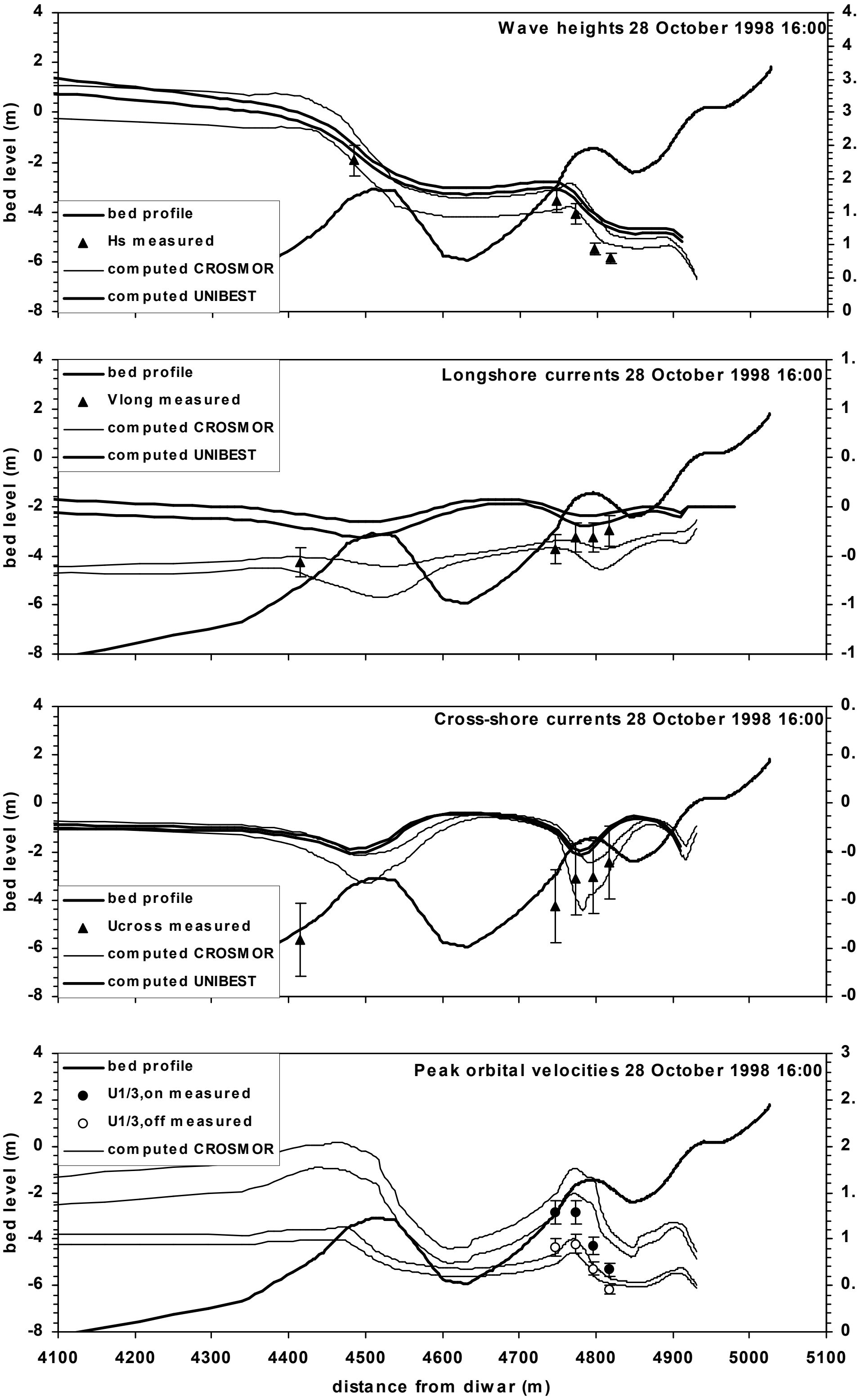

Figure 3 *Comparison of cross-shore distributions of wave height, longshore velocity and cross-shore velocity for Event 2 (28-10-1998 16:00).*

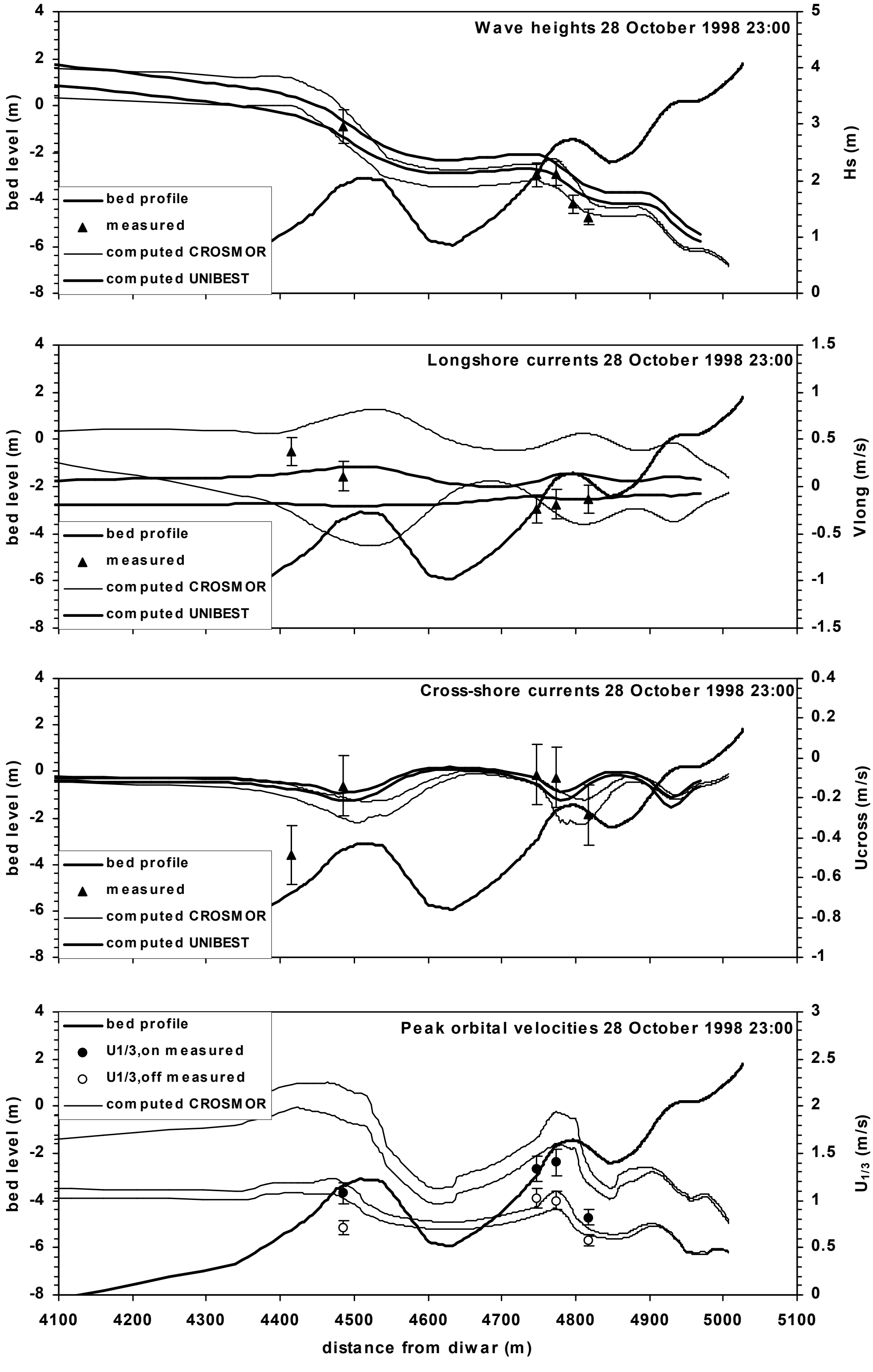

Figure 4 *Comparison of cross-shore distributions of wave height, longshore velocity and cross-shore velocity for Event 3 (28-10-1998 23:00).*

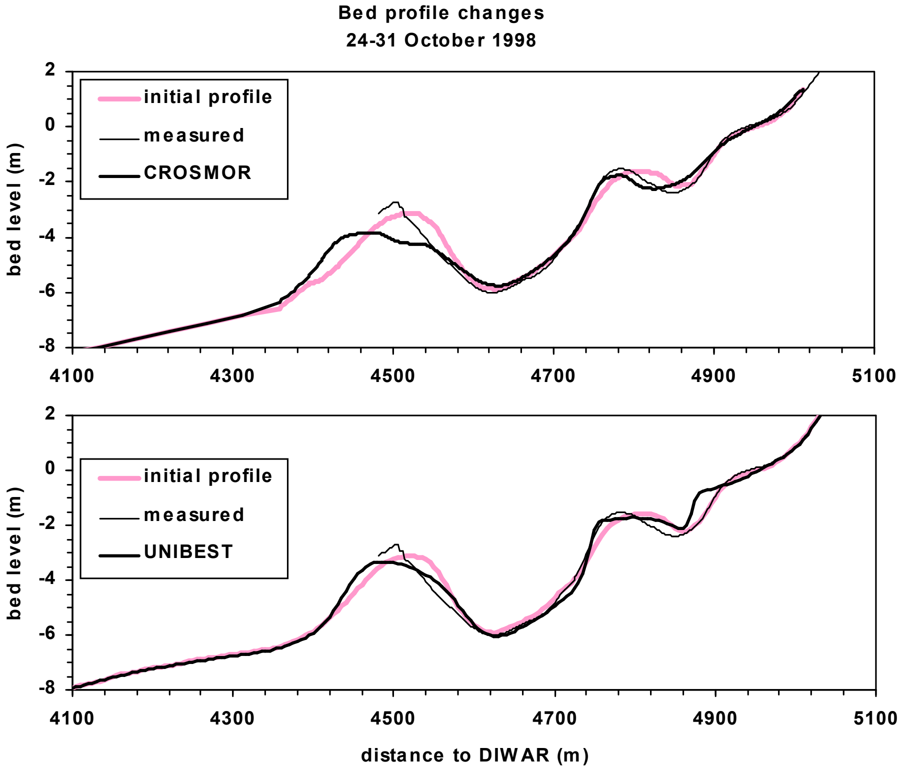

Figure 5 *Comparison of profile predictions during storm period 24-31 Oct.*

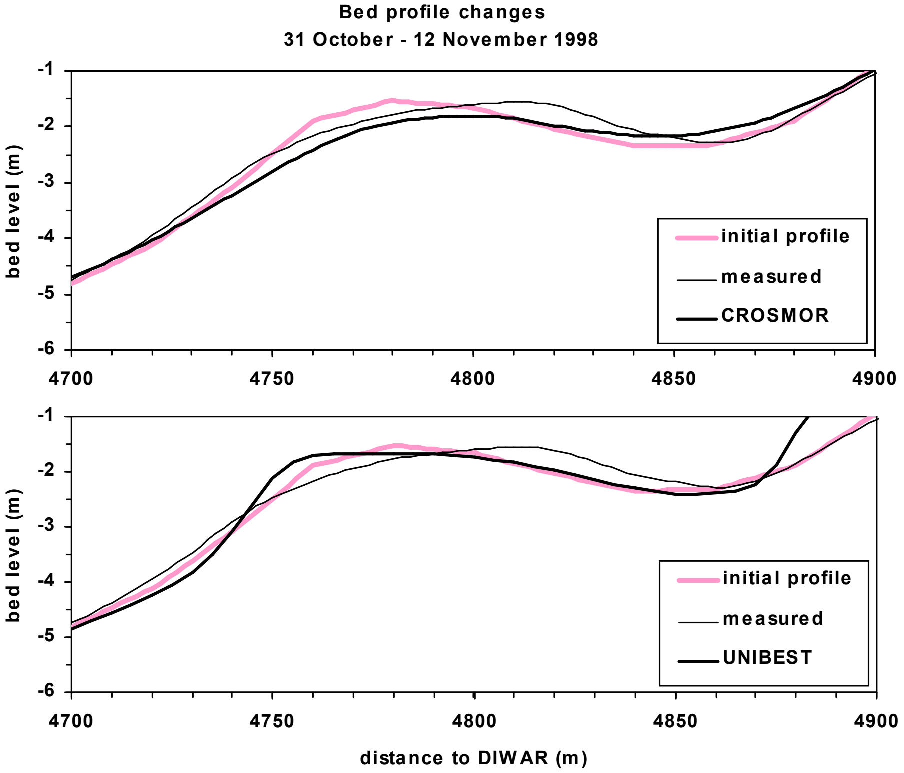

Figure 6 *Detail of inner bar during post-storm period 31Oct-12Nov.*